Available online at www.sciencedirect.com

SciVerse ScienceDirect

Procedia Engineering 31 (2012) 769 – 774

Procedia Engineering

www.elsevier.com/locate/procedia

International Conference on Advances in Computational Modeling and Simulation

Numerical Simulation of the Overall Flow Field for Underwater Vehicle with Pump Jet Thruster

Yongxiang Dong*, Xiangjie Duan, Shunshan Feng, Zhiyu Shao

State Key Laboratory of Explosion Science and Technology, Beijing Institute of Technology, Beijing 100081, China

Abstract

The flow field numerical simulation of underwater vehicle with pump jet thruster was performed using the commercially available CFD software FLUENT based on the Reynolds averaged Navier Stokes Equations and k-epsilon RNG turbulence model. Multiple reference frames (MRF) was used to associate the interior flow field of the pump jet thruster and exterior flow field of the underwater vehicle. Validity of the CFD model is verified using data from experiment. Characteristic of the overall flow field was obtained and pressure distribution of the propulsion was also given. The simulation results could be regarded as an important reference in the optimal design of pump jet thruster and the hydrodynamic characteristics of underwater vehicle.

Keywords: Pump jet thruster; Flow field with power; Hhydrodynamic characteristics; MRF

1. Introduction

Pump jet thrusters have been widely used as a propulsion device in underwater vehicle because of their excellent low noise characteristics [1]. The structural diagram of the underwater vehicle with pump jet thruster was showed in Fig 1. The pump jet thruster components include a rotor which rotates to obtain thrust, a stator prevents the rotation movement to offset the imbalance torque and a duct which protects the rotor and stator. The complicated structure of propulsion contributes to the complicated flow characteristics.

* Corresponding author. Tel.: +86-13683582319;
E-mail address: dongyongx@bit.edu.cn.

1877-7058 © 2011 Published by Elsevier Ltd. Open access under CC BY-NC-ND license.
doi:10.1016/j.proeng.2012.01.1100

Meanwhile, the wake flow field performance of underwater vehicle is affected by the pump jet thruster significantly. It results that hydrodynamic characteristics will be affected inevitably. Thus, research on overall flow field of underwater vehicle accelerated by pump jet thruster is of great significance. A few of the researchers has conducted the study of the interior flow field of pump jet thruster, as in [2][3]. But they focus on only interior flow field, few can provide the characteristics of the overall flow field includes both interior flow field and exterior flow field of the underwater vehicle, which is usually the most important to analyze the propulsion performance and its influence on the hydrodynamic characteristics of the underwater vehicle.

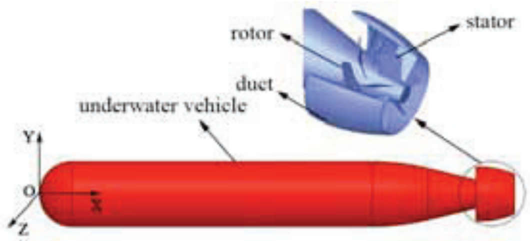

Fig. 1. Underwater vehicle accelerated by the pump jet thruster

In this paper, the multiple reference frames (MRF) is applied to associate the exterior flow field of underwater vehicle with the interior flow field of propulsion. Hybrid grid is used because of the structural complexity. The Fluent software is used to solve the RNAS equations with RNG k-ε turbulence model. The overall flow field of under vehicle with pump jet thruster is simulated .Comparison of the simulation results with a previously conducted full scale model experiment is performed, and the flow characteristic and the pressure distribution on the overall flow field with propulsion are given at last.

2. Flow Simulation Model of the Overall Flow

2.1. Physical Model and Mesh Generation

In a flow field simulation, computational domain selection is a key factor which determines the complexity and successfulness of the problem [4]. In our work, we are mainly concern how the flow in the interior of propulsion interacts with the exterior flow field of the underwater vehicle and its influence on hydrodynamic characteristics, so water in the interior of propulsion as well as outside of the underwater vehicle are both included in the computational domain. Due to the dissymmetry of the propulsion, 3D model must be used in the computation.

Schematic and boundary conditions of the longitudinal profile of the physical model is shown in Fig 2. Diameter of the underwater vehicle (referenced by d) was taken as a reference of the range of the flow field domain. Coordinate origin takes places at the vertex of the underwater vehicle head. The inlet, outlet, and wall boundary have an offset of $15d$, $35d$ and $15d$ respectively from the origin.

For the underwater vehicle, the fins and rudders were not modeled for the simplicity of the problem. To compare the hydrodynamic characteristics of with and without propulsion, the computational model with propulsion (referenced by B+P) and without propulsion (referenced by B) were respectively established.

The mesh generator used in this work is ICEM CFD. The computational domain was split into interior flow field and exterior flow field witch were showed in different color in Fig.2. For the structure complexity of the interior flow field, unstructured mesh was used. For the number of grids reduction and accuracy of the calculation, high quality structured mesh was used on the exterior flow field. The unstructured mesh and structured mesh have the same nodes at the interface so as to exchange the calculation information.

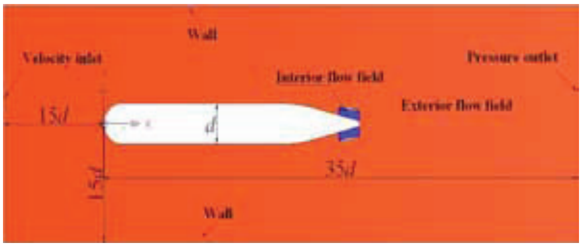

Fig. 2. Schematic and boundary conditions of the longitudinal profile of the physical model

2.2. Mathematical model

Reynolds averaged Navier Stokes Equations was used to govern the transport of the averaged flow quantities in consideration of the reduction of computational resources. The equations which been written in Cartesian tensor form is:

$$\frac{\partial U_j}{\partial x_j} = 0 \tag{1}$$

$$\rho \frac{\partial u_i}{\partial t} + \rho \frac{\partial u_i u_j}{\partial x_j} = -\frac{\partial P}{\partial x_j} + \frac{\partial}{\partial x_j}[\mu(\frac{\partial u_i}{\partial x_j} + \frac{\partial u_j}{\partial x_i}) - \frac{2}{3}\delta_{ij}\frac{\partial u_i}{\partial x_j}] + \frac{\partial}{\partial x_j}(-\rho \overline{u'_i u'_j})_i \tag{2}$$

Where ρ is the density and P is the Reynolds-averaged pressure, $U_{i,j}$ and $u_{i,j}$ is the fluid mean and fluctuating velocity components, μ is the dynamic viscosity. As it is well known the Reynolds stress tensor $\overline{u_i u_j}$ needs a closure and a popular one is based on the assumption of proportionality to the strain rate tensor, through a turbulent viscosity ν_t defined as

$$\nu_t = \frac{\mu_t}{\rho} = C_\mu \frac{k^2}{\varepsilon} \tag{3}$$

k is the turbulent kinetic energy and ε is the turbulent kinetic energy dissipation rate. In the present investigation the standard k-ε model was used and two additional equations were introduced:

$$U_j \frac{\partial k}{\partial x_j} = \frac{1}{\rho}\frac{\partial}{\partial x_j}\left[\left(\mu + \frac{\mu_t}{\sigma_k}\right)\frac{\partial k}{\partial x_j}\right] + P_k - \varepsilon \tag{4}$$

$$U_j \frac{\partial \varepsilon}{\partial x_j} = \frac{1}{\rho}\frac{\partial}{\partial x_j}\left[\left(\mu + \frac{\mu_t}{\sigma_\varepsilon}\right)\frac{\partial \varepsilon}{\partial x_j}\right] + C_{\varepsilon 1}\frac{\varepsilon}{k}P_k - C_{\varepsilon 2}\frac{\varepsilon^2}{k} \tag{5}$$

Where the turbulent kinetic energy production term P_k can be written as follows,

$$P_k = \nu_t \left(\frac{\partial U_i}{\partial x_j} + \frac{\partial U_j}{\partial x_i}\right)\frac{\partial U_i}{\partial x_j} \tag{6}$$

In the equations above $C_\mu, C_{\varepsilon 1}, C_{\varepsilon 2}, \sigma_k, \sigma_\varepsilon$ are model constants and the values:

$$C_\mu = 0.09,\ C_{\varepsilon 1} = 1.45,\ C_{\varepsilon 2} = 1.90,\ \sigma_k = 1,\ \sigma_\varepsilon = 1.3$$

2.3. Numerical Solver and Boundary conditions

The commercially available CFD solver FLUENT was used in this simulation. In the computation the pressure based implicit steady solver is used and the pressure-velocity coupling algorithm is SIMPLEC. For accuracy second order method was used for pressure, momentum and the turbulence viscosity discretization.

The MRF is a steady-state approximation in which individual cell zones can be assigned different rotational or translational speeds. The flow in each moving cell zone is solved using the moving reference frame equations. If the zone is stationary (ω=0), the equations reduce to their stationary forms. In our work, the interior flow field sub zone needs a rotational speed to realize the rotor rotation and exterior flow field just be assigned a zero rotational speed because it is stationary.

For the boundary conditions, the underwater vehicle, duct and stator are stationary wall boundary relative to the exterior flow field. The rotor is moving wall relative to exterior flow field and its rotational speed is the same as the interior flow field. The inlet and outlet of the overflow field are given velocity inlet and pressure outlet respectively to realize a uniform flow field with a constant speed.

3. Results

Comparison of the simulation results with a previously conducted full scale model experiment is showed in Fig 3. As can be seen in Fig 3, the thrust results of the propulsion show good agreement between simulation and experiment corresponding to different rotational speed of the rotor. The CFD model of the flow field for underwater vehicle with pump jet thruster has been verified.

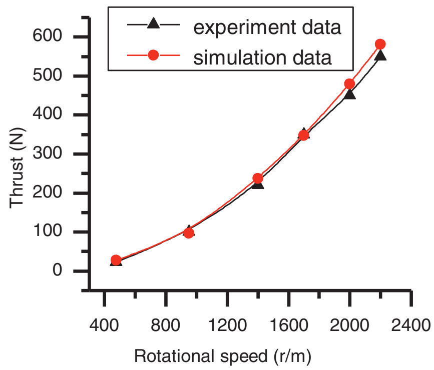

Fig. 3. The comparison of pump jet thruster thrust between experimental and simulation

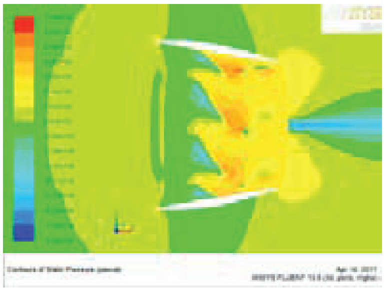

Fig. 4. Pressure distribution of pump jet thruster interior field

Fig 4 shows the contour plot of pressure field of the interior flow field of the propulsion. From Fig 4, we can see that thrust side of the rotor has a high pressure and suction side of the rotor has a low pressure. This is why the propulsion can provide the thrust.

As is known that the poor propulsion performance could course a bad effect on the hydrodynamic characteristics of the underwater vehicle [5]. Fig 5 shows the pitching moment coefficient comparison of within (referenced by B+P) and without (referenced by B) propulsion. The pitching moment coefficient at different angle of attack reduces 3% generally after the propulsion was concerned. From the figure we can found that the propulsion has little effect on the stability of the underwater vehicle. That is, the propulsion in this paper has a good design.

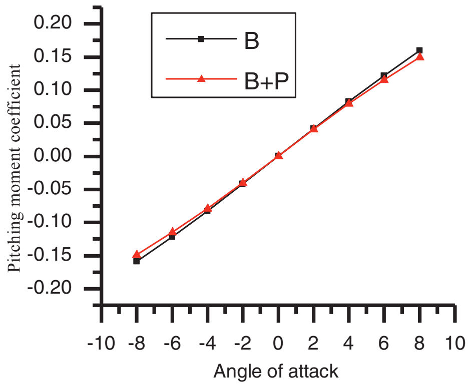

Fig. 5. Comparison of pitching moment coefficient between model B and model B+P

4. Conclusion

From this study of CFD application, we can conclude that the overall flow field of underwater vehicle with pump jet thruster can be well simulated by multiple reference frames (MRF) of FLUENT. Through analyzing the flow field, it has been found that Lift coefficient and pitch moment coefficient changed less than 3%. The simulation results could be regarded as an important reference in the optimal design of pump jet thruster and the hydrodynamic characteristics of underwater vehicle.

References

[1] Tiansen LI. Torpedo Manoeuvrability;2007.

[2] Jingping. XIAO, Hua. JIN. Power effect research on torpedo model with counter-rotation pusher propeller. *Experiments and Measurements in Fluid Mechanics* 2001;15:3.

[3] Zhirong ZHANG, Baiqi LI. Integral calculation of viscous flow around ship hull with propeller. *Journal of Ship Mechanics* 2004;8:5.

[4] Zhihua LIU, Ying XIONG, Jinming Ye. Study on the prediction of propeller open-water performance using RANS formula and multi-block hybrid meshes. *Journal of hydrodynamics* 2007;22:4.

[5] Tao ZHANG, Chenjun YANG, Baowei SONG. Investigationson the numerical simulation method forthe open-water performance of contra-rotatingpropellers based on the MRF model. *Journal of Ship Mechanics* 2010;14:8.